Mechanical properties of self-irradiated single-crystal copper*

Li Wei-Na(李维娜)[a], Xue Jian-Ming(薛建明)[b)c)†], Wang Jian-Xiang(王建祥)[a], and Duan Hui-Ling(段慧玲)[a)c)‡]

[a] *State Key Laboratory for Turbulence and Complex System, Department of Mechanics and Aerospace Engineering, College of Engineering, Peking University, Beijing* 100871, *China*

[b] *State Key Laboratory of Nuclear Physics and Technology, School of Physics, Peking University, Beijing* 100871, *China*

[c] *Key Laboratory of High Energy Density Physics Simulation, Center for Applied Physics and Technology, Peking University, Beijing* 100871, *China*

(Received 10 May 2013; revised manuscript received 4 August 2013; published online 24 January 2014)

Molecular dynamics simulations are performed to investigate the influence of irradiation damage on the mechanical properties of copper. In the simulation, the energy of primary knocked-on atoms (PKAs) ranges from 1 to 10 keV, and the results indicate that the number of point defects (vacancies and interstitials) increases linearly with the PKA energy. We choose three kinds of simulation samples: un-irradiated and irradiated samples, and comparison samples. The un-irradiated samples are defect-free, while irradiation induces vacancies and interstitials in the irradiated samples. It is found that due to the presence of the irradiation-induced defects, the compressive Young modulus of the single-crystal Cu increases, while the tensile Young modulus decreases, and that both the tensile and compressive yield stresses experience a dramatic decrease. To analyze the effects of vacancies and interstitials independently, the mechanical properties of the comparison samples, which only contain randomly distributed vacancies, are investigated. The results indicate that the vacancies are responsible for the change of Young modulus, while the interstitials determine the yield strain.

Keywords: irradiation damage, single crystal, mechanical property, molecular dynamics simulation

PACS: 61.80.–x, 61.82.Bg, 62.20.–x, 02.70.Ns **DOI:** 10.1088/1674-1056/23/3/036101

1. Introduction

Copper and its alloys are the most popular materials used in nuclear facilities, and the irradiation effects in these materials have been studied for a long time. In view of practical applications, investigation of the degradation to the mechanical properties induced by irradiation is crucially important because the mechanical properties are related to the service time and safety of the nuclear facility.

As is well known, the irradiation of metals and alloys induces defect formation[1–3] and a change of mechanical properties.[4–6] Most significant radiation damage at low radiation temperatures increases yield stress and flow stress (known as the hardening effect), dramatic embrittlement, loss of work hardening, and plastic instability. The phenomena are believed to be caused by the interactions between the radiation-induced defect clusters and material microstructures, such as grown-in dislocations and grain boundaries. To develop anti-irradiation materials for future nuclear facilities, we must understand the degradation of the mechanical properties of metals under irradiation.

Irradiation can induce microstructure evolution, which can affect the mechanical properties of materials, such as vacancy loops, tetrahedral, and voids.[7,8] In the early stage of irradiation (<ns), the main formations of irradiation-induced defects are vacancies and self-interstitial atoms (SIAs). Thus, understanding how vacancies and SIAs influence the mechanical properties of metals has an implication on the mechanism of irradiation damage.

Recently, molecular dynamics (MD) simulations have been testified to be an effective way to study mechanical properties of metals,[9–11] and also has been widely used to investigate irradiation damage behaviors in materials caused by energetic particles.[12–20] In the present paper, MD method is employed to simulate defect production in single crystal Cu and to examine how the mechanical properties change due to the irradiation produced point defects. Our results are very helpful to understand the mechanical properties of metals in the early stage of irradiation.

2. Simulation methods

As shown in Fig. 1(a), our simulation model for the single-crystal copper has the shape of a rectangular parallelepiped with size of $14a\times14a\times40a$, where a (= 0.3615 nm) is the lattice parameter. The simulation sample contains 10240 atoms in an FCC structure. The x, y, z axes are chosen as [100], [010], and [001] directions, and periodic boundary conditions are used in all the three directions. Initially, the sample is maintained at 300 K and relaxes for 200 ps under NPT ensemble to equilibrium.

To simulate the primary knock-on atom (PKA) irradia-

*Project supported by the National Basic Research Program of China (Grant No. 2011CB013101) and the National Natural Science Foundation of China (Grant Nos. 11172001, 91226202, and 11225208).

†Corresponding author. E-mail: jmxue@pku.edu.cn

‡Corresponding author. E-mail: hlduan@pku.edu.cn

© 2014 Chinese Physical Society and IOP Publishing Ltd

tion, one atom is chosen and given a specified kinetic energy. Figure 1(b) shows that the chosen PKA irradiates with an angle of 15° with respect to the y axis, thus avoiding the channeling effect. Twelve different PKA energies ranging from 0.5 keV to 10 keV are used in the simulation to investigate the energy effect on the copper properties. During the PKA movement, the NVE ensemble is used and the time step varies from 0.05 fs (at the beginning of the collision) to 1 fs. After the PKA stops, the samples are cooled down to 300 K and fully relaxed under NVT ensemble to equilibrium.

Finally, the irradiated samples are stretched (compressed) along the z axis by increasing (decreasing) the sample size along the z axis l_z repeatedly. At each loading step, l_z is changed by 0.2%, then the samples are relaxed at 300 K for 40 ps. The stress is calculated using the Virial theorem and each value is averaged over 20 ps.

The embedded atom method (EAM) potential developed by Minishet *et al.*[21] is used to describe the interaction between copper atoms in the simulation, because it gives accurate defect formation energy and stacking fault energy for Cu. When the inter-atom distance is smaller than 0.5 Å, the Ziegler–Biersack–Littmark (ZBL) potential[22] is used instead of the EAM potential to describe the repulsive interactions between the recoil atom and target atoms. The MD simulations are performed using LAMMPS.[23]

The influence of irradiation on single-crystal Cu is studied by comparing the mechanical properties (Young's modulus, yield strain, and yield stress) of the un-irradiated (defect-free) Cu sample and those of irradiated ones. Since irradiation induces vacancies and interstitials during the collision cascade, comparison samples with randomly distributed vacancies are also investigated to distinguish the effect of the vacancies from that of interstitials on the mechanical properties.

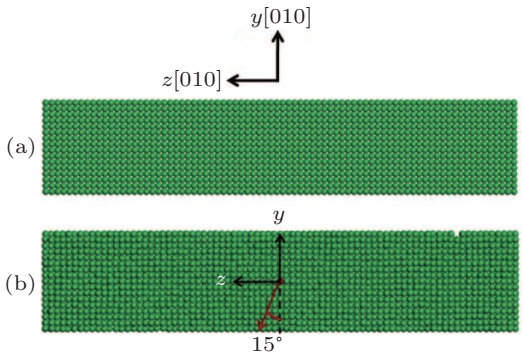


Fig. 1. (color online) Atomistic model of the single crystal Cu. (a) Sample cutted at 0 K. (b) Equilibrium configuration at 300 K. The chosen PKA irradiates with an angle of 15° with respect to the y axis, thus avoiding the channeling effect.

Uniaxial strain is applied to the un-irradiated single-crystal Cu, the obtained stress-strain curves are given in Fig. 2(a). For both tension and compression, the stress increases with the increase of strain until a critical point is reached, then the Cu sample yields with the decrease of stress. To compare the elastic behaviors of Cu under tension and compression, we plot Fig. 2(b) with the absolute stress and strain values before yield. Two phenomena in Fig. 2(b) are noticeable. First, for a small strain, Cu deforms elastically and the magnitude of stress increases linearly with the increase of strain; when strain exceeds 2%, the stress–strain relationship quickly becomes nonlinear, especially for the compression. Second, single-crystal Cu yields at a smaller strain under compression, which makes the compressive yield stress (−3.95 GPa) much smaller than the tensile yield stress (9.72 GPa).

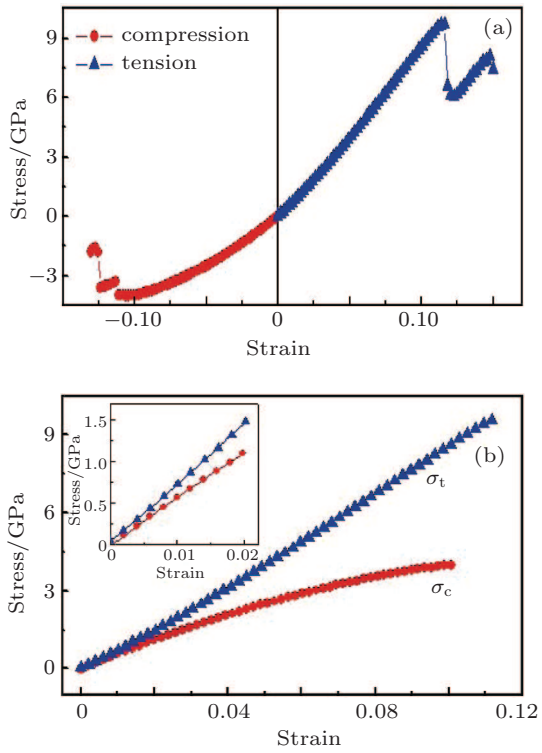


Fig. 2. (color online) (a) Stress–strain curve of a single-crystal Cu at 300 K and (b) the absolute values of strain and stress for comparing the nonlinearity under compression and tension. The inset in panel (b) shows the fitting to expression $\sigma = E\varepsilon + D\varepsilon^2$.

To obtain the Young's modulus E, stress–strain curves are fitted using equation: $\sigma = E\varepsilon + D\varepsilon^2$, where D is the higher-order elastic modulus. To reduce the nonlinear effect on E, the data for strains $|\varepsilon| < 2\%$ are used in the fitting. The obtained tensile and compressive Young's moduli are $E_t = 65.57$ GPa and $E_c = 62.00$ GPa, respectively. The subscripts t and c denote the tension and compression, respectively. A smaller E_c is found on single-crystal Cu because of the nonlinear effect. These results accord well with the *ab initio* calculations[24] and MD simulations using another EAM potential.[25]

For the nonlinear effect under compression, we think it involves the slip system activated during yielding. It is known that FCC metal deforms plastically via dislocation slip. The slip plane is the close-packed {111} plane, and slip directions

are the close-packed orientations: $\langle 112 \rangle$ and $\langle 110 \rangle$. When the shear stress along a slip direction reaches a critical resolved shear stress (CRSS), the slip system is activated and yield happens. Thus, dislocations tend to slip along the direction with the largest shear stress. In material, there are "hard" orientations and "soft" orientations, where "hard" or "soft" measures the probability with which the slip happens along such a direction. Let ϕ denote the angle title from the loading direction. "Hard" orientation has $\phi = 0^\circ$ or 90°, shear stress along any of such directions is zero and the corresponding slip system will not be activated. "Soft" orientation has $\phi = 45^\circ$, and the shear stress along the direction is the largest, and dislocations tend to slip along the direction. As shown in Fig. 3(a), the loading direction is [001] in our simulation and the green arrow denotes the "soft" direction with the largest shear stress. The [110] direction is the "hard" direction ($\phi = 90^\circ$) with zero shear stress, so the slip system $\{111\}\langle 110 \rangle$ cannot be activated and only the $\{111\}\langle 112 \rangle$ partial slip can happen when the shear stress reaches CRSS. Under tension, the [112] slip direction rotates away from the "soft" direction, which makes the yield difficult and further loading is needed to activate the slip system. Under compression, the [112] slip direction rotates towards the "soft" direction. This makes the yield easy under a rather small load. This leads to a large tensile yield stress and a small compressive yield stress.

Common neighbor analysis (CNA)[26,27] is performed to visualize the defects after yields. Figures 3(b) and 3(c) show the atomic configurations after yield under compression and tension. The FCC atoms are shown in green, while the stacking fault atoms and non-twelve coordinated atoms are shown in red and grey. Single crystal Cu yields via the $\{111\}\langle 112 \rangle$ partial slip, which leaves the stacking faults in the slipped area.

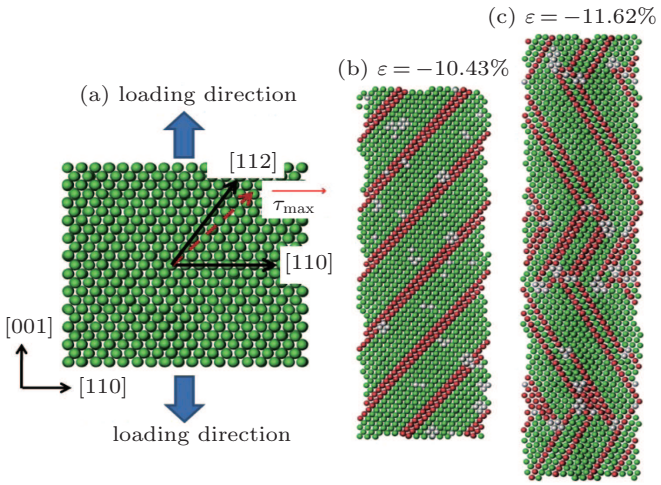


Fig. 3. (color online) (a) Loading direction, slip directions, and the "soft" orientation τ_{max}. (b) and (c) Atomic configurations after yield under compression and tension. Atoms are colored based on the crystal structure. Green and red denote FCC atoms and stacking faults atoms, respectively, while the non-twelve coordinated atoms are shown in grey.

Next, we study the influence of irradiation on the mechanical properties of a single crystal Cu sample. The irradiation induces the point defects, namely vacancies and interstitials, which are counted by the Wigner–Seitz cell method, and the results are shown in Fig. 4. Clearly, the number of vacancies increases linearly with the increase of PKA energy and this tendency accords with the prediction from the NRT formula: $n = 0.8E_k/(2/E_d)$, where E_k is the PKA energy, and E_d is the minimum energy needed for an atom to be displaced. Since the irradiation mechanism of Cu has been widely investigated, we do not discuss in detail the irradiation damage of Cu here.

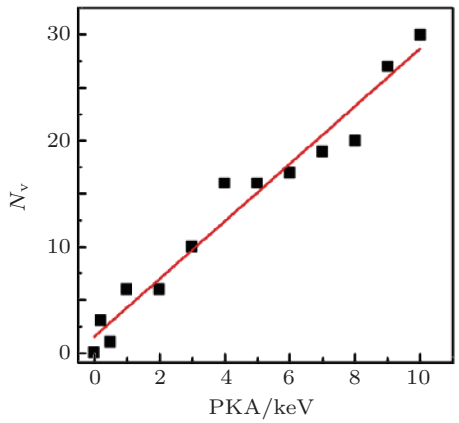


Fig. 4. (color online) Number of vacancies varying with PKA energy.

The stress–strain curves for the irradiated and unirradiated Cu samples are shown in Fig. 5, where the data after yield are not given. The largest stress and smallest stress on each curve give the yield stresses under tension and compression. Compared with the original Cu sample, all the irradiated Cu samples have the small yield stresses.

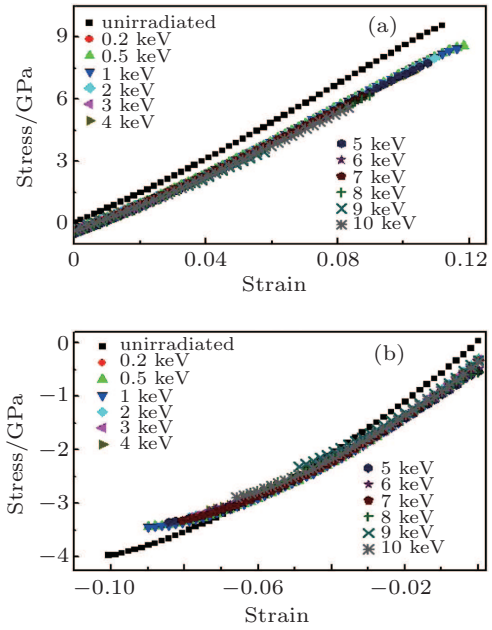


Fig. 5. (color online) Stress–strain curves for irradiated and unirradiated Cu under tension (a) and compression (b).

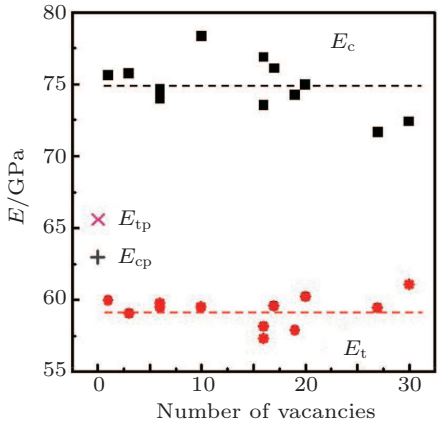


Fig. 6. (color online) Young moduli for irradiated and un-irradiated Cu varying with the number of vacancies, with E_{tp} and E_{cp} denoting the tensile and compressive Young modulus for un-irradiated Cu. Dashed lines are drawn to guide the eyes.

To obtain the Young's modulus E, the stress–strain curves for strains $|\varepsilon| < 2\%$ are fitted to expression $\sigma = E\varepsilon + D\varepsilon^2$. Figure 6 shows the variations of tensile and compressive Young's moduli for the un-irradiated and irradiated samples with the number of vacancies. The sample with zero vacancies refers to the un-irradiated Cu, and the compressive Young's modulus E_{cp} is slightly smaller than the tensile Young's modulus E_{tp}. For the irradiated samples, we find that the compressive Young's modulus E_c is larger than E_{cp}, while the tensile Young's modulus E_t is smaller than E_{tp}, and E_c is always larger than E_t. For the cases with less than 30 vacancies, neither E_t nor E_c shows any obvious dependence on the number of vacancies.

As analyzed above, the irradiation induces the same number of vacancies and interstitials in Cu samples, which results in the change of Young's modulus as shown in Fig. 6. To figure out how vacancies and interstitials play a role in changing the mechanical properties of single-crystal Cu, in the following we investigate the mechanical property of the comparison sample, which only contains point vacancies.

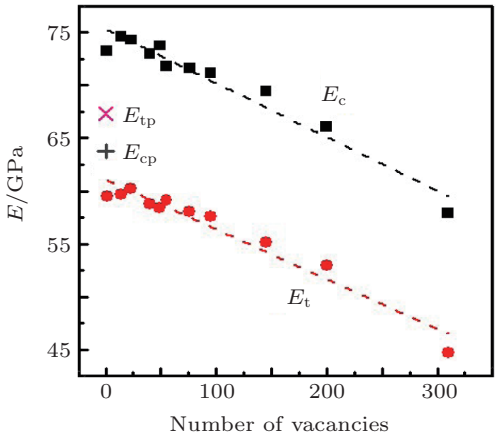


Fig. 7. (color online) Plots of Young's moduli for comparison samples versus the number of vacancies, with E_{tp} and E_{cp} denoting the tensile and compressive Young's modulus for un-irradiated Cu. Dashed lines are used only to guide the eyes.

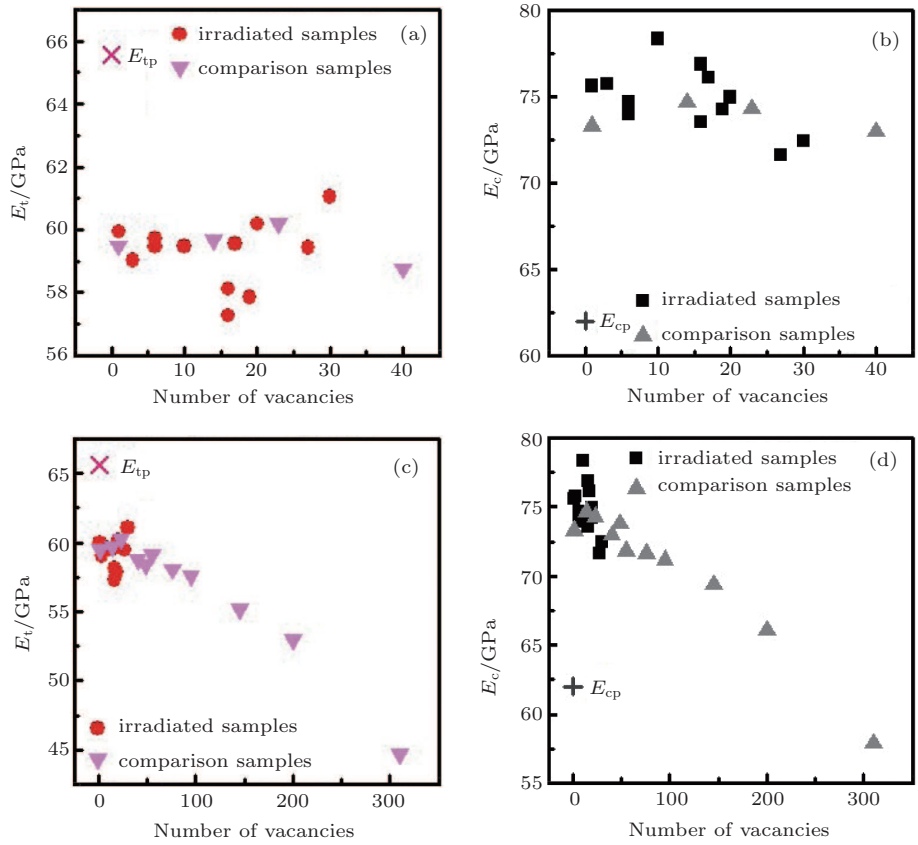


Fig. 8. (color online) (a) and (c) Tensile Young's moduli; (b) and (d) compressive Young's moduli of irradiated and comparison samples.

The comparison samples are generated by deleting randomly chosen atoms, and the eleven samples with vacancies from 1 to 310 are simulated. Uniaxial strains are applied to these vacancy samples, and figure 7 shows the variation of the Young's moduli with the number of vacancies.

We can see that E_t decreases with the number of vacancies while E_c first increases then decreases. When a few vacancies appear in the single-crystal Cu, E_c increases rapidly with the number of vacancies and achieves its maximal value (74.64 GPa) at 14 vacancies. As more vacancies appear, E_c shows a linear decrease with the number of vacancies increasing. With 310 vacancies (vacancy density $\sim 3\%$), E_t decreases by 32% while E_c only decreases by 7%. Figure 8 shows the comparisons of the Young's modulus between irradiated samples and comparison samples. It can be seen that the Young's moduli of both kinds of Cu samples have the same trend when the samples have the same number of vacancies.

Figure 9 shows the comparison of yield stress and yield strain between irradiated samples and comparison samples. For the comparison sample, both yield stress and yield strain decrease linearly with the number of vacancies. Dashed lines give the linear fitting to the data. It can be seen that with the same number of vacancies, yield stresses and yield strains of irradiated samples are much smaller than those of comparison samples. Note that there are two kinds of point defects in irradiated samples, i.e., interstitials and vacancies, which always exist in pairs. Interstitials induce lattice distortion and local shear stress, both of which tend to activate the slip systems at small strains. This could be the reason why small yield strains are found to appear on irradiated samples. Even though the compressive Young's modulus E_c increases after irradiation, the compressive yield stress σ_c has a decrease in its magnitude as has the tensile yield stress σ_t. Yield stress depends on yield strain, and the nonlinear effect and irradiation cause a huge decrease in yield strain which dominates over the value of yield stress.

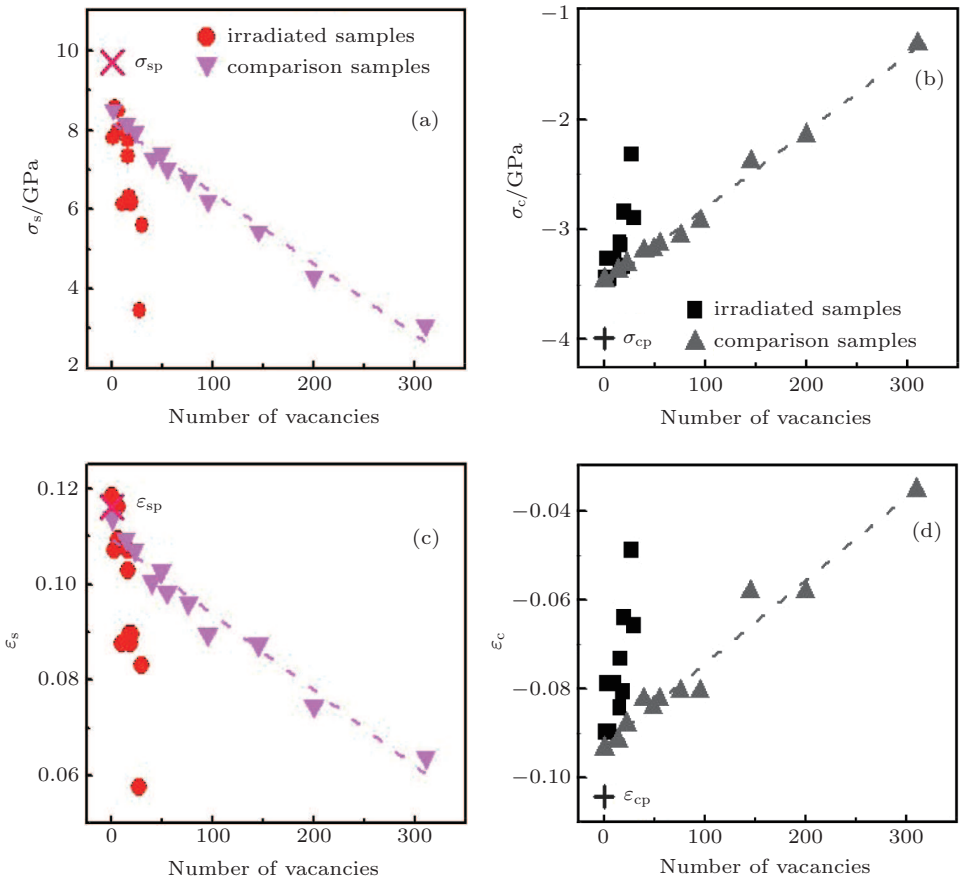


Fig. 9. (color online) Comparisons of yield stress ((a) and (b)) and yield strain ((c) and (d)) between irradiated and comparison samples. σ_{tp} and σ_{cp} denote the tensile and compressive yield stress for un-irradiated Cu, while ε_{tp} and ε_{cp} refer to the tensile and compressive yield strain, respectively. Dashed lines give the linear fitting to the data obtained from comparison samples.

Figure 10 shows the atomic stress σ_{zz} of the Cu sample irradiated by 10 keV ions. We observe that the atomic stress is not homogeneous and larger stress magnitudes are at defects (vacancies, interstitials). The existence of these defects lowers the stress threshold to nucleate a dislocation and dislocations tend to nucleate at these defects. Figure 9 shows that the irradiated samples have smaller yield strains than the comparison samples. The comparison samples only contain point vacan-

cies, while defect clusters appear in the irradiation samples. Dislocations tend to nucleate at vacancy clusters which have concentrated local stress and offer free room for nucleation.

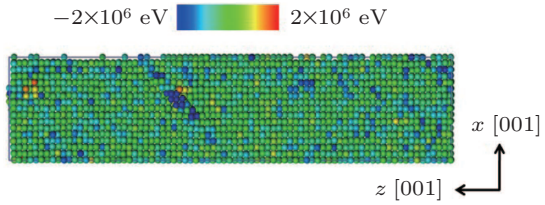


Fig. 10. (color online) Atomic configuration of the sample (irradiated by 10 keV ions) just about to yield under compression. Atoms are colored to show the variation of atomic stress along the strain direction σ_{zz}.

The radiation-hardened effect is observed in experiment, that is, metal gains a larger yield stress after irradiation. For the experimental samples, lots of dislocations have been introduced during fabrication process, and irradiation defects tend to interact with these grown-in dislocations and impede dislocation motion. Thus, a higher stress is needed to activate the dislocation, and makes the experimental sample yield. In addition, our simulation samples are pure single crystals and defect-free. After irradiation, irradiation defects bring in stress concentration and offer free volume for dislocation nucleation. We observe that the dislocations nucleate and slip in the irradiated samples at a lower loading, which results in a decrease in yield stress.

We examine the mechanical properties of irradiated single-crystal Cu, and find that the irradiation-induced defects reduce the tensile Young's modulus, but increase the compressive Young's modulus. The comparison samples with randomly-distributed vacancies are also studied. It is found that the Young's moduli of irradiated samples and comparison samples share similar values while yield stresses of irradiated samples are much smaller than those obtained from comparison samples. It is believed that the irradiation-induced interstitials increase the local shear stress, which can easily activate the slip system at small strains, thus resulting in a small yield strain.

3. Summary

We perform MD simulations to investigate the effect of the irradiation on the mechanical properties of single-crystal Cu. Uniaxial strains are applied to the un-irradiated and irradiated Cu, and mechanical properties, such as the Young's modulus, yield strain, and yield stress, are analyzed. Some conclusions are drawn below.

(i) Irradiation induces point defects in single-crystal Cu, namely, vacancies and interstitials, which exist in pairs. The number of vacancies increases with the increase of PKA energy.

(ii) After irradiation, the tensile Young's modulus decreases, while the compressive Young's modulus increases.

(iii) By studying the comparison samples with random vacancies, it is found that the tensile Young's modulus decreases with increasing number of vacancies, while the compressive Young's modulus first increases then decreases.

Acknowledgment

Huiling Duan would like to thank the Alexander von Humboldt (AvH) foundation in Germany for supporting this work through project "Mechanics Theory of Materials with Complex Surfaces and its Applications" in the frame of the AvH program for funding a research group linkage.

References

[1] Caturla M J, Soneda N, Alonso E, Wirth B D, de la Rubia T D and Perlado J M 2000 *J. Nucl. Mater.* **276** 13
[2] Zinkle S J and Singh B N 2000 *J. Nucl. Mater.* **283** 306
[3] Domain C, Becquart C S and Malerba L 2004 *J. Nucl. Mater.* **335** 121
[4] Singh B N, Foreman A J E and Trinkaus H 1997 *J. Nucl. Mater.* **249** 103
[5] Singh B N, Horsewell A, Toft P and Edwards D J 1995 *J. Nucl. Mater.* **224** 131
[6] Odette G R, Yamamoto T, Rathbun H J, He M Y, Hribernik M L and Rensman J W 2003 *J. Nucl. Mater.* **323** 313
[7] Zinkle S J and Singh B N 1993 *J. Nucl. Mater.* **199** 173
[8] Singh B N and Zinkle S J 1993 *J. Nucl. Mater.* **206** 212
[9] Wolf D, Yamakov V, Phillpot S R, Mukherjee and Gleiter H 2005 *Acta Mater.* **53** 1
[10] Meyers M A, Mishra A and Benson D J 2006 *Prog. Mater. Sci.* **51** 427
[11] Lee J C, Park K W, Kim K H, FleuryE, Lee B J, Wakeda M and Shibutani Y 2007 *J. Mater. Res.* **22** 3087
[12] Bacon D J, Calder A F, Gao F, Kapinos V G and Wooding S J 1995 *Nucl. Instrum. Methods Phys. Res. B* **102** 37
[13] Bacon D J and Delarubia T D 1994 *J. Nucl. Mater.* **216** 275
[14] Calder A F and Bacon D J 1993 *J. Nucl. Mater.* **207** 25
[15] Stoller R E 1996 *J. Nucl. Mater.* **233** 999
[16] StollerR E, Odette G R and Wirth B D 1997 *J. Nucl. Mater.* **251** 49
[17] Becquart C S, Domain C, van Duysen J C and Raulot J M 2001 *J. Nucl. Mater.* **294** 274
[18] Zou X Q, Xue J M and Wang Y G 2010 *Chin. Phys. B* **19** 036102
[19] Li W N, Sun L X, Xue J M, Wang J X and Duan H L 2013 *Nucl. Instr. Meth. B* **307** 158
[20] Sun L X, Lan C E, Zhao S J, Xue J M and Wang Y G 2012 *J. Phys. D: Appl. Phys.* **45** 135403
[21] Mishin Y, Mehl M J, Papaconstantopoulos D A, Voter A F and Kress J D 2001 *Phys. Rev. B* **63** 224106
[22] Ziegler J F, Biersack J P and Littmark U 1985 *The Stopping and Range of Ions in Matter* (New York: Pergamon)
[23] Plimpton S J 1995 *J. Comput. Phys.* **117** 1
[24] Cerny M, Sob M, Pokluda J and Sandera P 2004 *J. Phys.: Condens. Matter* **16** 1045
[25] Milstein F and Chantasiriwan S 1998 *Phys. Rev. B* **58** 6006
[26] Honeycutt J D and Andersen H C 1987 *J. Phys. Chem.* **91** 4950
[27] Stukowski A 2012 *Modell. Simul. Mater. Sci. Eng.* **20** 045021